UNCLASSIFIED

Defense Technical Information Center Compilation Part Notice

ADP012392

TITLE: Tunable Diode Laser Gain Measurements of the HF[2-0] Overtone Transitions in a Small Scale HF Laser

DISTRIBUTION: Approved for public release, distribution unlimited

This paper is part of the following report:

TITLE: Gas and Chemical Lasers and Intense Beam Applications III Held in San Jose, CA, USA on 22-24 January 2002

To order the complete compilation report, use: ADA403173

The component part is provided here to allow users access to individually authored sections of proceedings, annals, symposia, etc. However, the component should be considered within the context of the overall compilation report and not as a stand-alone technical report.

The following component part numbers comprise the compilation report:
ADP012376 thru ADP012405

UNCLASSIFIED

Tunable Diode Laser Gain Measurements of the HF(2-0) Overtone Transitions in a Small Scale HF Laser

Charles F. Wisniewski[a], Gerald C. Manke II*[a], Gordon D. Hager[a],
Peter G. Crowell[b], and C. Randall Truman[c].
[a]Air Force Research Laboratory, Directed Energy Directorate; [b]Logicon/Northrup Grumman;
[c]Department of Mechanical Engineering, University of New Mexico.

ABSTRACT

A tunable diode laser was used to probe the overtone gain medium of a small-scale HF laser. Two-dimensional, spatially resolved small signal gain and temperature maps were generated for the P(3) ro-vibrational transition in the first HF overtone band.

1. INTRODUCTION

The fundamental HF laser was invented in the mid to late 1960's[1-5]. While the first HF lasers were pulse initiated[2-5], continuous wave HF lasers were also demonstrated prior to 1970[6-8]. Over the last 30 years, HF laser technology has advanced to the point where megawatt class lasers can be constructed. It is widely recognized that the fundamental HF laser, which operates from 2.7 - 3.0 μm, has limited utility for low altitude, long-range propagation applications due to strong absorptions in the atmosphere. Subsonic demonstrations of HF overtone lasers, which operate at a wavelength that is more amenable to long-range, low-altitude applications, were first reported in the mid-1970's by Hon[9] and Bashkin[10]. However, the demonstrations were not particularly impressive due to poor efficiency. A more modern and scalable concept for an HF overtone laser was demonstrated in 1984 by Jeffers[11]. This demonstration was especially notable because of the significantly enhanced efficiency; the overtone power was 20 - 30% of the fundamental. Improved mirrors and combustion driven HF laser technology were the keys to demonstrations of multi-kW HF overtone lasers in the mid- to late-1980's[12-14]. In general, the small signal gain of an HF overtone laser is approximately 2 orders of magnitude smaller than the fundamental HF laser. The development and scaling of the HF overtone lasers (i.e. $\Delta v = -2$) has been limited by the availability of mirror coatings which simultaneously suppress fundamental lasing and enable overtone oscillation. As the ability to produce such optics has improved, so too have the prospects of high-power HF overtone lasers.

Another impediment to the development of HF overtone lasers has been the lack of high fidelity small signal gain probes that can be used to directly measure the small signal gain of individual HF ro-vibrational lines with full spectral and spatial resolution. While it is possible to use a commercial Helios arc-driven HF laser as a probe, this device can be difficult and expensive to operate. In most cases, the Helios laser cavity is stabilized and locked to the line center of one of a limited number of HF overtone lines. Alternatively, a plot of extracted laser power vs. mirror reflectivity can be used to determine the threshold gain (g_{th}) according to the equation

$$g_0 = g_{th} = -\frac{1}{2L}\ln R_1 R_2 \qquad [1]$$

where R_1 and R_2 are the mirror reflectivities and L is the path length. As the outcoupling mirror reflectivity decreases and the outcoupled power approaches zero the small signal gain (g_0) equals the threshold gain. However, this technique cannot generate spatially resolved gain or temperature maps. Since the efficiency of an HF laser is usually dominated by the rate of mixing, the need for spatial resolution is acute. Furthermore, this method cannot be used to measure gain on individual ro-vibrational lines because the measured threshold gain is only associated with the strongest line in the multi-line overtone spectrum. Finally, neither of these techniques can provide information about the gas temperature or any other data related to the spectral lineshape of the transition.

In principle, the lack of precise lineshape information may lead to ambiguous or deceptive answers when making comparisons with computational fluid dynamics calculations. In particular, while the gain of a laser may be directly measured, extraction of the inversion density requires knowledge of the spectral lineshape function. The definition of gain is

$$gain(cm^{-1}) = \ln\left(\frac{I(v_0)}{I_0(v_0)}\right)z^{-1} = \sigma_{stim}(v_0)\left[N_u - \frac{g_u}{g_l}N_l\right] \qquad [2]$$

Gas and Chemical Lasers and Intense Beam Applications III, Steven J. Davis, Michael C. Heaven, Editors, Proceedings of SPIE Vol. 4631 (2002) © 2002 SPIE · 0277-786X/02/$15.00

where z is the optical path length and N_u, N_l, g_u, and g_l are the upper and lower state number densities and degeneracies, respectively. The stimulated emission cross section is given by

$$\sigma_{stim}(v_0) = \frac{\lambda^2 A(v,J)}{8\pi} f(v_0) \quad [3]$$

where λ is the center wavelength, A(v, J) is the Einstein emission coefficient, and $f(v_0)$ is the lineshape function. If the lineshape is assumed to be Gaussian, and is actually a Voigt or some other more complex function, the calculated value for the inversion density may be significantly in error. Pressure broadening coefficients (2γ) for HF[15, 16] range from 0.75 MHz Torr^{-1} for HF + He to 53.05 MHz Torr^{-1} for HF + HF. Under most HF supersonic laser conditions (low pressure, mostly He), pressure broadening is not an issue, but an explicit check for it would be prudent.

Because of their narrow linewidth and tunability, External Cavity Diode Lasers (ECDLs) are ideal tools for measuring small signal gain. These devices have previously been implemented for measuring the gain in the Chemical Oxygen Iodine Laser (COIL)[17] and the All Gas-phase Iodine Laser (AGIL)[18]. In fact, the same commercially available (New Focus, model 6300) 1.3-micron diode laser used for AGIL and COIL was also used to measure gain on our HF overtone laser test bed. As we have done in the past[17, 18], we have generated spatially resolved, small signal gain and temperature maps of the active medium for comparison with CFD modeling results[19].

2. EXPERIMENTAL METHODS

A small-scale HF laser was constructed to generate an inversion on the first overtone of HF at 1.27 - 1.40 μm. The laser consisted of a 5 cm wide supersonic slit nozzle, where F atoms generated by a Helios discharge tube reacted with molecular hydrogen to generate vibrationally excited HF[20]. Our nozzle design and experimental conditions are very similar to those of Sentman and co-workers[21, 22]. The two most important differences are that we used a slit nozzle rather than a nozzle bank, and our discharge used 20% F_2 in helium rather than SF_6 + O_2 as the F atom source. Schematic representations of our experimental apparatus are shown in Figure 1a-b. Figure 1b shows the view from the downstream end of the nozzle looking into the plenum region. Helium is added through the first row of injection holes, while the second row was used for the addition of H_2. The injected helium acts as a shield for the injected H_2, with the goal of preventing reaction prior to the nozzle exit plane. A pair of He shroud flows were placed at the nozzle exit plane (NEP) to reduce recirculation of the laser media and a pair of bank blowers were located on either side of the active medium to reduce expansion of the corrosive gas flow into the mirror tunnels. The 0.9 cm long slit nozzle expands from the 3 mm throat with a 20 degree angle (relative to the center line) to 0.9 cm at the NEP. The nozzle design also provides for area relief via a large 1 cm step (top and bottom) at the NEP. A small base purge flow of He could be added to prevent recirculation in the base region.

A Helios DC discharge tube was used to generate a flow of fluorine atoms from molecular fluorine (20% in He, Matheson) diluted in helium. High purity H_2(99.99%, Matheson) and He (Air Products) were added without additional purification. Table 1 lists the typical range of reagent flow rates, device pressures and thermocouple temperatures. The plenum pressure was typically 24 Torr and the static pressure (measured at the wall 3 cm downstream of the NEP) was ~2 Torr. A series of pitot tube measurements established the Mach number and total pressure, ~2.5 and 20 Torr, respectively.

The diode laser used to probe the absorption/gain on the HF(v = 0) → HF(v = 2) vibrational transition has been described previously[18, 23, 24]. In this case, the laser was tuned to individual HF ro-vibrational lines instead of the $I(^2P_{3/2})$ - $I^*(^2P_{1/2})$ spin-orbit transition. The frequency of the laser was repetitively scanned over approximately 6GHz at a 50Hz rate. The I/I_0 signal was averaged for approximately 1 second (i.e. 50 scans) to improve the signal to noise ratio.

Spatially resolved emission spectra were generated with a 0.3 m Acton monochromator and a Near Infrared Optical Multi-channel Analyzer (NIR OMA) (Roper Scientific, OMA V). The 512 pixel array of InGaAs detectors generates the spectra with resolution well suited for our application. Fiber optic bundles were used to deliver the chemiluminescence to the monochromator. The small solid angle viewed by lens attached to the fiber optic bundle allows for spatially resolved emission spectra. While the lens - flow reactor separation used in these experiments does not allow resolution of the vertical profile, we can easily resolve the streamwise profile in 2 - 3 cm steps.

3. RESULTS AND DISCUSSION

A typical HF overtone gain measurement is shown in Figure 2. The HF(2-0) P(3) line was chosen because it should have the highest gain at our experimental conditions (H_2 = 27 mmols sec^{-1}, F_2, = 1 mmols sec^{-1}, P(static) = 1.5 Torr, and T ~ 200 K). For the sake of clarity, only every other data point is shown. The peak gain is 0.07 % cm^{-1} and

the peak width (FWHM) = 515 MHz. Also shown in Figure 2 is the Gaussian lineshape function fit to the data. The residuals for the Gaussian fit are shown in the lower panel. Note that the residuals plot has no structure, indicating that no pressure-related line broadening or narrowing effects are evident[15, 16]. The spectral linewidth corresponds to T = 198 K.

Figures 3a - 3c show spatially resolved small signal gain measurements. The data were generated by moving the diode laser along the vertical (y) and streamwise (x) axes of the reactor. To reduce the number of experiments, we assumed symmetry across the centerline. Hence, the data points below the centerline are identical to the measured values from above the centerline. Each panel corresponds to one of three positions along the x-axis (1, 5, and 9 cm downstream, relative to the NEP) and the three sets of data in each panel correspond to one of three H_2 flow rates (5, 10, or 27 mmols sec^{-1}). The solid vertical lines in each panel indicate where the top and bottom base purge regions begin. For x = 1 cm downstream of the NEP, the gain peaks at approximately the same position (relative to the centerline) as the H_2 injectors. This strongly suggests that molecular hydrogen has not penetrated into the center of the flow stream. The double peaked profile is less pronounced but still persists 5 cm downstream of the NEP. At x = 9 cm, the peak gain is along the centerline of the flow, demonstrating that, albeit somewhat slowly, the H_2 does eventually penetrate into the center of the flow. The vertical profiles at 1 and 5 cm downstream show significant expansion of the flow into the base purge regions.

The highest observed small signal gain was ~0.1 % cm^{-1}. This result compares well with the results of Sentman and coworkers' Parallel Slit Nozzle (PSN)[25-27] and HYSIM lasers[21, 22]. It is important to note, however, that in both cases they did not directly measure the small signal gain. Rather, they report the product g_0L_e, (where L_e is the effective path length) based on plots of the outcoupled power vs. mirror reflectivity. In the case of the PSN device, if an effective path length of 14.9 cm is assumed for the PSN device (i.e. the path length predicted by CFD calculations of the size of the active medium), then the small signal gain is 0.085 % cm^{-1}. If, on the other hand, the geometric path length (30 cm) is used, the small signal gain is a factor of 2 smaller. Our result (which assumes L = 5 cm for our slit nozzle) is more consistent with Sentman if we adopt the assumption that L_e = 14.9 cm. Considering the strong similarties between our hardware and Sentman's, the apparent agreement with our result is not surprising.

Figure 4 shows the corresponding spatial temperature measurements. The uncertainty of the temperature in most cases is substantial because the signal to noise ratio is poor, and the lineshape is ill defined. In such cases where a reliable linewidth is not possible, only the small signal gain (which depends on the spectral area) is reported. In general, the temperature varies approximately 100 K from the centerline to the middle of the base purge region, peaking where the gain is highest.

The small signal gain was probed for several lines in addition to P(3). Figure 5 shows a few examples for HF(2-0) P(2) and P(4). While chemiluminescent spectra indicate that positive gain may also exist on several HF(3-1) lines, we could not directly probe these transitions due to the limited frequency range of the diode laser. Emission spectra of the flow at z = 1 - 12 cm are shown in Figure 6. According to the Boltzmann equation,

$$\ln\left[\frac{Intensity(v,J)}{A(v,J)*g(J)}\right]=\frac{-B_v*[J*(J+1)]}{kT} \qquad [3]$$

(where B_v is the rotational constant) a plot of the left hand side vs. J(J+1) is linear if rotational equilibrium exists, and the slope is equal to B_v/kT. A linear plot was obtained for each vibrational level, and the temperatures are indicated in panels a-e. The vibrational distribution is also indicated. The relative vibrational population is calculated from equations [4]

$$P(v)=\frac{I(v,J)}{P(J)*A(V,J)} \qquad [4]$$

and [5]

$$P(J)=\frac{g(J)*\exp(-Bv*[J*(J+1)]/kT)}{Q_{rot}} \qquad [5]$$

where Q_{rot} is the rotational partition function. The rotational temperatures are slightly higher than, but not inconsistent with the spectroscopically determined translational temperatures. Both types of temperature tend to increase slightly as the flow progresses downstream. Finally, we note that the vibrational distribution for P_2 - P_5 also relaxes along the length of the reactor.

4. CONCLUSIONS

A tunable diode laser has been used to measure the small signal gain of a small-scale supersonic HF overtone laser. Unlike previous measurements of the overtone gain, our technique is direct, and can be both spatially and spectrally resolved. This data is complemented by spatially resolved overtone emission spectra that confirm that each vibrational state is in rotational equilibrium. These data are ideal for 2D and 3D computational fluid dynamics (CFD) calculations. When combined with the results of the CFD calculations[19], this experiment should represent the most comprehensive characterization and analysis of an HF overtone laser reported to date.

5. ACKNOWLEDGMENTS

The authors wish to acknowledge helpful discussions with Prof. L. H. Sentman regarding the construction and operation of the HYSIM nozzle, Prof. R. K. Hanson (Stanford University) for advice on HF overtone lineshape analysis, Dr. D. L. Carroll (CU Aerospace, LLC) regarding advice on preliminary CFD calculations, and Applied Research Associates, Inc. for computer time used to perform the preliminary CFD calculations. We are especially grateful to Brian Anderson (AFRL/DE) for assistance with the diode laser.

6. REFERENCES

1. Rolf W. F. Gross and Jerry F. Bott, *Handbook of chemical lasers*, Wiley, New York, 1976.
2. K. L. Kompa and G. C. Pimentel, *J. Chem. Phys.*, **47**, 857, 1967.
3. T. F. Deutsch, *Appl. Phys. Lett.*, **10**, 234, 1967.
4. O. M. Batovskii, G. K. Vasil'ev, E. F. Makarov and V. L Tal'rose, *JETP Lett.*, **9**, 200, 1969.
5. N. G. Basov, L. V. Kulakov, E. P. Markin, A. I. Nikitin and A. N. Oraevsky, *JETP Lett.*, **9**, 375, 1969.
6. R. W. F. Gross, R. R. Giedt and T. A. Jacobs, *J. Chem. Phys.*, **51**, 1250, 1969.
7. J. R. Airey and S. F. McKay, *Appl. Phys. Lett.*, **15**, 401, 1969.
8. D. J. Spencer, T. A. Jacobs, H. Mirels and R. W. F. Gross, *Int. J. Chem. Kinet.*, **1**, 493, 1969.
9. J. F. Hon and J. R. Novak, "Chemically pumped hydrogen fluoride overtone laser", *IEEE J. Quant. Elect.*, **QE-11**, 698 - 699, 1975.
10. A. S. Bashkin, V. I. Igoshin, Yu. S. Leonov, A. N. Oraevskii and O. E. Porodinkov, "An investigation of a chemical laser emitting due to an overtone of the HF molecule", *Sov. J. Quantum Electron.*, **7**, 626 - 627, 1977.
11. W. Q. Jeffers, "Short Wavelength Chemical Lasers", *AIAA Journal*, **27**, 64 - 66, 1988.
12. W. Duncan, S. Patterson, B. Graves and M. Holloman, "Recent Progress in Hydrogen Fluoride Overtone Chemical Lasers", AIAA-91-1480, 1991.
13. W. Duncan, M. Holloman, B. Rogers and S. Patterson, "Hydrogen Fluoride Overtone Chemical Laser Technology", AIAA-89-1903, 1989.
14. W. A. Duncan, S. P. Patterson, M. E. Holloman and J. L. Sollee, Progress in Hydrogen Fluoride Overtone Chemical Lasers, 1990
15. S. I. Chou, D. S. Baer and R. K. Hanson, "Diode laser measurements of He-, Ar-, and N2-broadened HF lineshapes in the first overtone band", *J. Mol. Spectrosc.*, **196**, 70-76, 1999.
16. S. I. Chou, D. S. Baer and R. K. Hanson, "Spectral Intensity and lineshape measurements in the first overtone band of HF using tunable diode lasers", *J. Mol. Spectrosc.*, **195**, 123-131, 1999.
17. R. F. Tate, B. S. Hunt, C. A. Helms, K. A. Truesdell and G. D. Hager, "Spatial Gain Measurements in a Chemical Oxygen Iodine Laser (COIL)", *IEEE J. Quant. Elect.*, **31**, 1632 - 1636, 1995.
18. J. M. Herbelin, T. L. Henshaw, B. D. Rafferty, B. T. Anderson, R. F. Tate, T. J. Madden, G. C. Manke and G. D. Hager, "The measurement of gain on the 1.315 μm transition of atomic iodine in a subsonic flow of chemically generated NCl($a^1\Delta$)", *Chem. Phys. Lett.*, **299**, 583-588, 1999.
19. C. F. Wisniewski, G. C. Manke II, G. D. Hager, C. R. Truman and P. F. Crowell, "in preparation", 2002.
20. G. C. Manke II and G. D. Hager, "A Review of Recent Experiments and Calculations Relevant to the Kinetics of the HF Laser", *J. Phys. Chem. Ref. Data*, **30**, 713 - 733, 2001.
21. L. H. Sentman, A. J. Eyre, J. T. Cassibry and B. P. Wootton, "Studies of cw HF Chemical Laser Performance", AAE TR 99-01, UILU ENG 99-0501, 1999.
22. L. H. Sentman, A. J. Eyre, B. P. Wootton and J. T. Cassibry, "Comparison of cw HF Laser Performance for Several Nozzles", AIAA 99-3469, 1999.
23. G. C. Manke II, T. L. Henshaw, T. J. Madden, J. M. Herbelin, B. D. Rafferty and G. D. Hager, "Characterizing fluorine and chlorine atom flow rates using iodine atom spectrometry", *AIAA Journal*, **39**, 447 - 454, 2001.

24. Thomas L. Henshaw, Gerald C. Manke II, Timothy J. Madden, Michael R. Berman and Gordon D. Hager, "A new energy transfer chemical laser at 1.315 μm", *Chem. Phys. Lett.*, **325**, 537 - 544, 2000.
25. L. H. Sentman, P. T. Theodoropoulos, T. Nguyen, D. L. Carroll and R. E. Waldo, "An Economical Supersonic cw HF Laser Testbed", AIAA Paper 89-1898, 1989.
26. D. L. Carroll, L. H. Sentman, P. T. Theodoropoulos, R. E. Waldo and S. J. Gordon, "Experimental Study of Continuous Wave Hydrogen-Fluoride Chemical Laser Overtone Performance", *AIAA Journal*, **31**, 693 - 700, 1993.
27. D. L. Carroll, L. H. Sentman, P. T. Theodoropoulos, R. E. Waldo, S. J. Gordon and J. W. Otto, "Experimental and Theoretical Study of cw HF Chemical Laser Overtone Performance", AAE TR 92-02, UILU ENG 92-0502, 1992.

Table 1: Typical Experimental Conditions

Parameter	Range
Flow Rates	
F_2	1 mmols sec^{-1}
H_2	0 - 30 mmols sec^{-1}
He(primary)	90 mmols sec^{-1}
He(secondary)	15 mmols sec^{-1}
He(base purge)	15 mmols sec^{-1}
Cavity Pressure, Temperature	
Pressure (static)	1.5 - 2.0 Torr
Pressure (total)	~20 Torr
Temperature (plenum / cavity wall)	370 / 290 K
Mach #	2.1 - 2.4

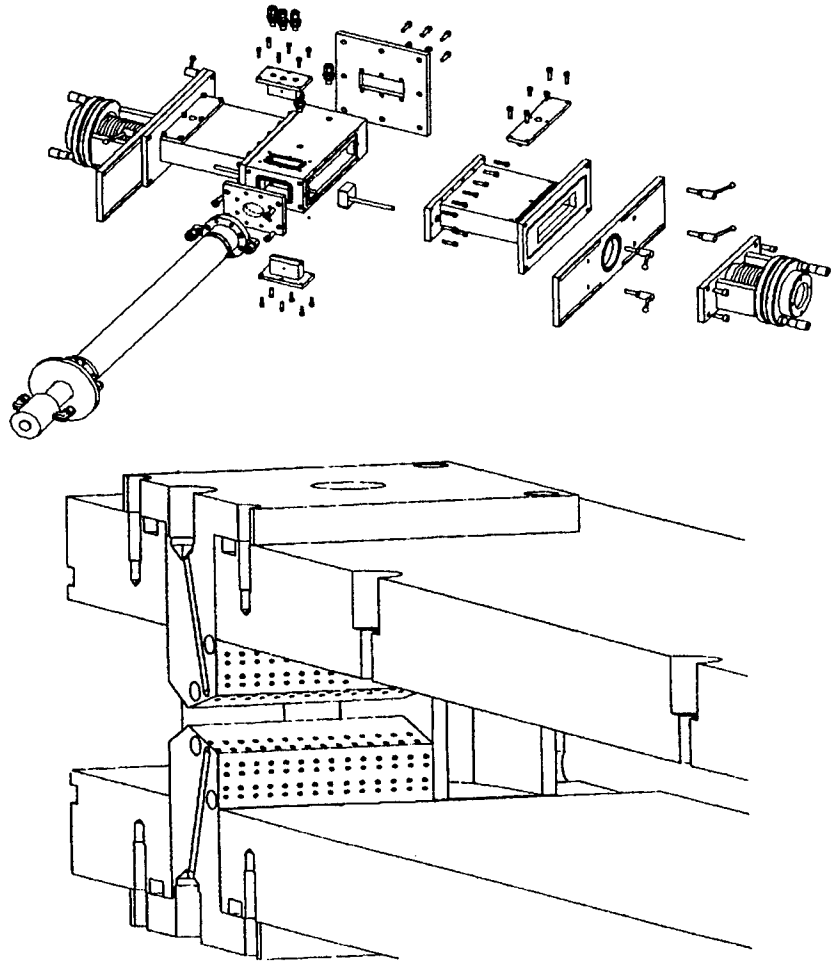

Figures 1a & 1b. HYSIM slit nozzle configuration. **(a).** A construction diagram for the HYSIM slit nozzle is shown. Fluorine atoms are generated by the DC discharge and enter the plenum region before passing through the 3 mm high slit nozzle. Laser mirrors or glass windows can be mounted along the sides of the reactor to accommodate laser demonstrations or gain measurements, respectively. **(b).** Downstream view of the supersonic slit nozzle. The first two rows of injectors just downstream of the slit are for secondary (trip jet) He and H_2 injection, respectively. A 1 cm step (top and bottom) occurs at the Nozzle Exit Plane (NEP), 0.9 cm downstream of the nozzle throat. Additional He is added to purge this region and prevent recirculation.

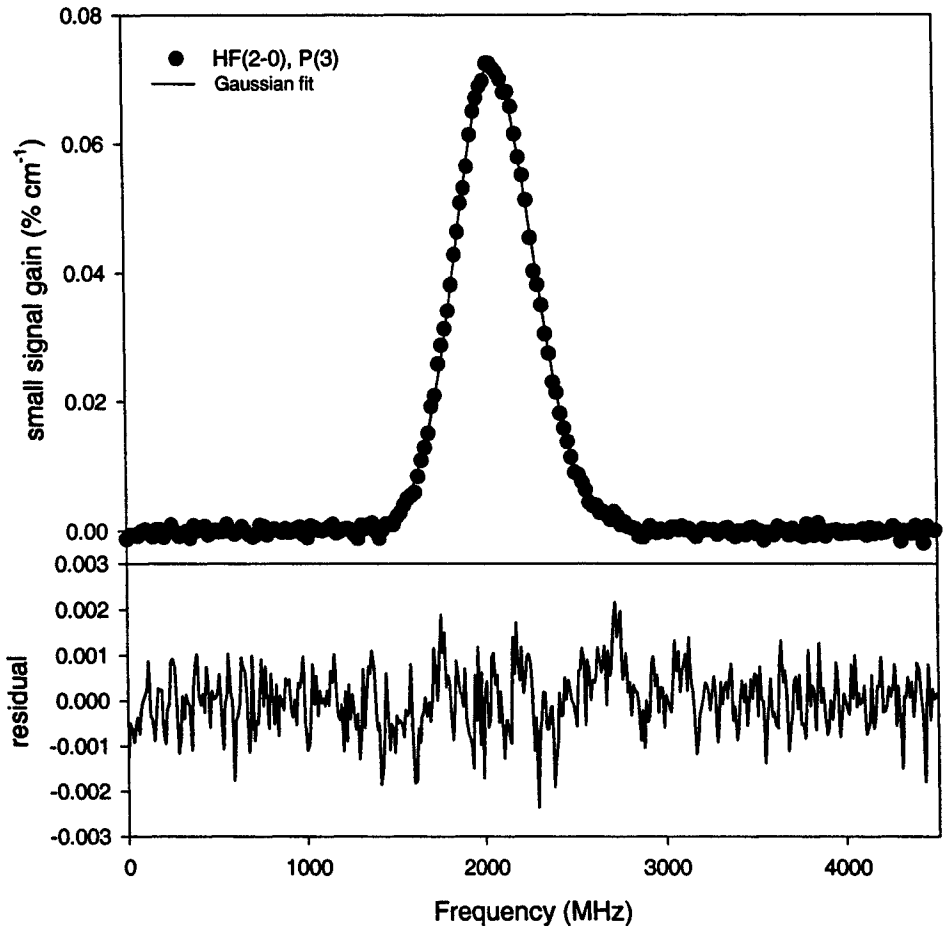

Figure 2. Small signal gain on HF(2-0) P(3). A sample HF overtone small signal gain spectrum is shown. The experimental conditions for the upper panel are F_2 = 1 mmol sec^{-1}, H_2 = 27 mmols sec^{-1}, P ~ 2 Torr, x = 5 cm downstream of the NEP, and y = 0.25 cm above the centerline. For purposes of clarity, only every other data point is shown. The spectrum is fit by a Gaussian function which gives area = 39.6, width(FWHM) = 515.2 MHz, and peak gain = 0.072 % cm^{-1}. The linewidth corresponds to T = 198 K. A residual plot is shown in the lower panel, demonstrating that the Gaussian line function adequately fits the entire lineshape. If pressure broadening had been present, the residual plot would have non-random structure.

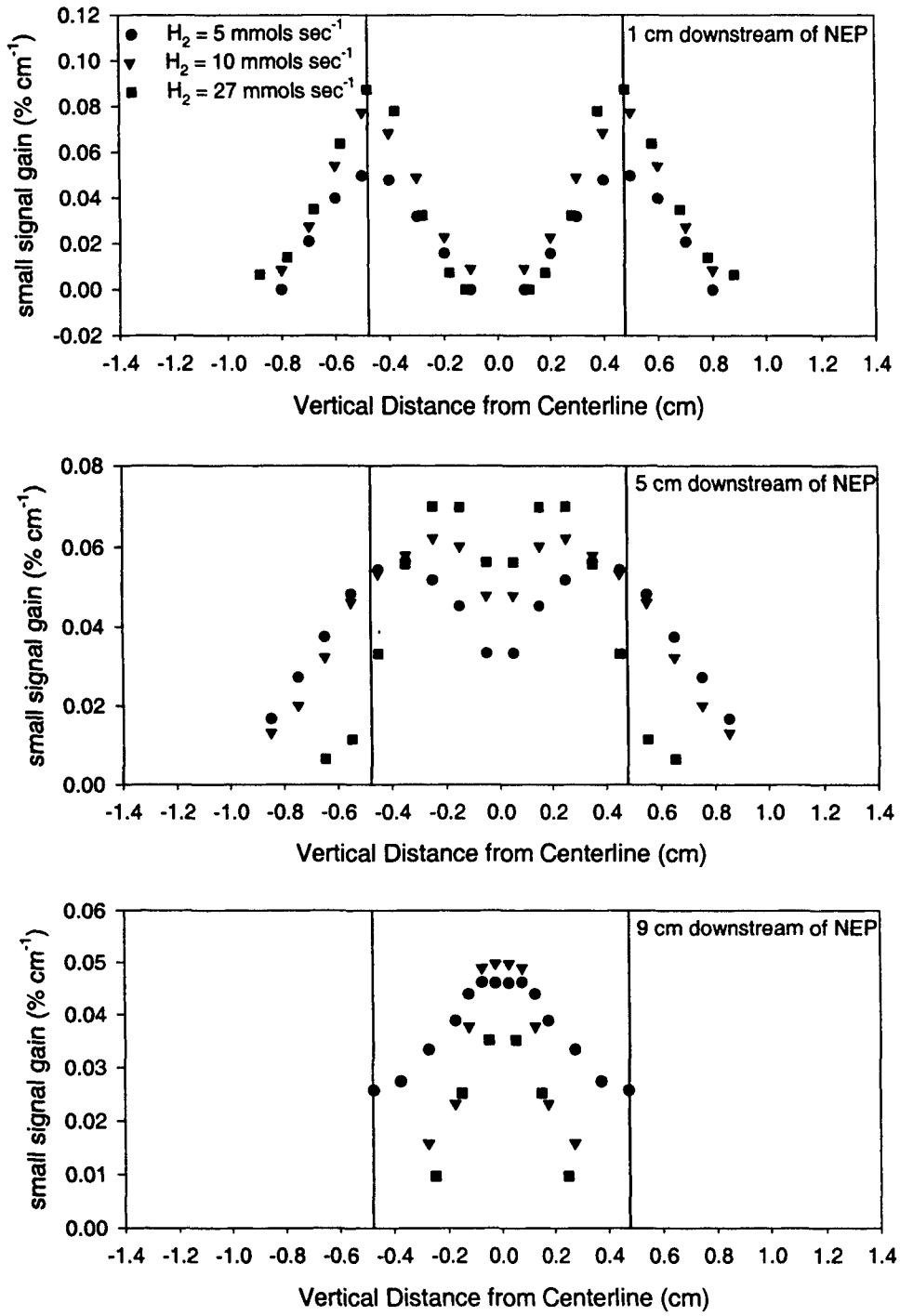

Figures 3a-c. Vertical small signal gain profiles. The diode probe laser was scanned along the vertical (y) and streamwise (x) axes of the reactor. The solid lines indicate the edges of the top and bottom base purge regions. The vertical small signal gain profile measured 1 cm downstream of the NEP indicates poor penetration of hydrogen and significant expansion of the flow into the base purge region. The mixing into the center of the flow channel improves as the flow marches downstream of the NEP, but the peak gain decreases from 0.08 % cm^{-1} at 1 cm to 0.05 % cm^{-1} at 9 cm.

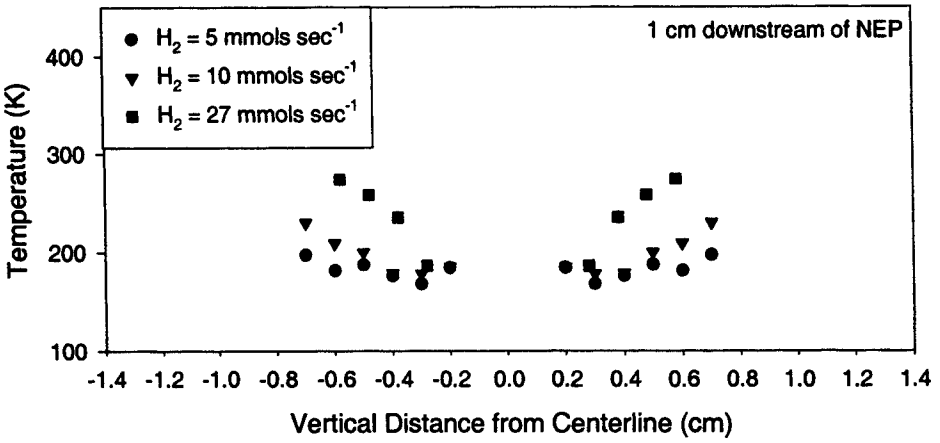

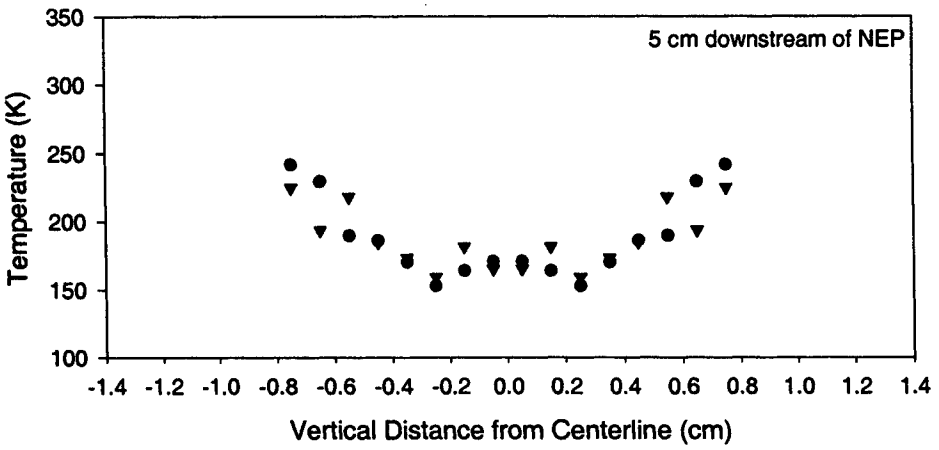

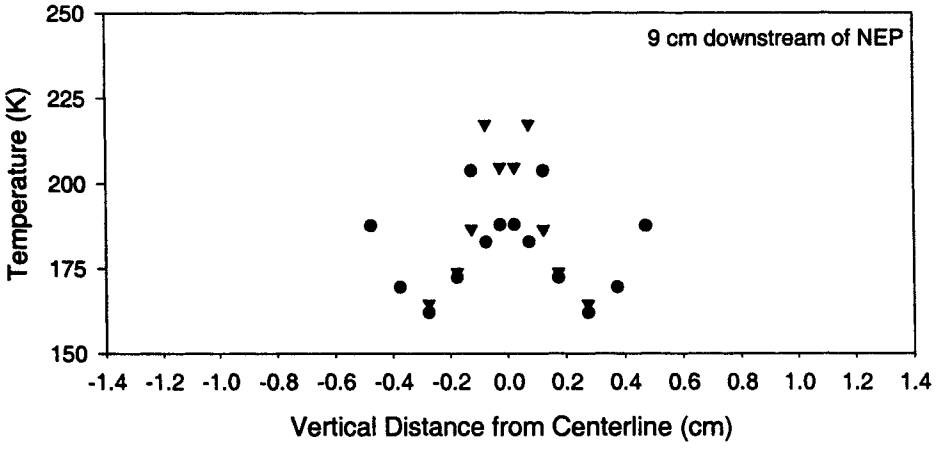

Figures 4 a - c. Vertical temperature profiles. The diode probe laser was scanned along the vertical (y) and streamwise (x) axes of the reactor. The uncertainty of the temperature in some cases is substantial because the signal to noise ratio is poor and a reliable peak width could not be determined. Hence, fewer data points appear than in Figures 3 a-c. The temperature varies approximately 100 K from the centerline to the middle of the base purge region, peaking where the gain is highest.

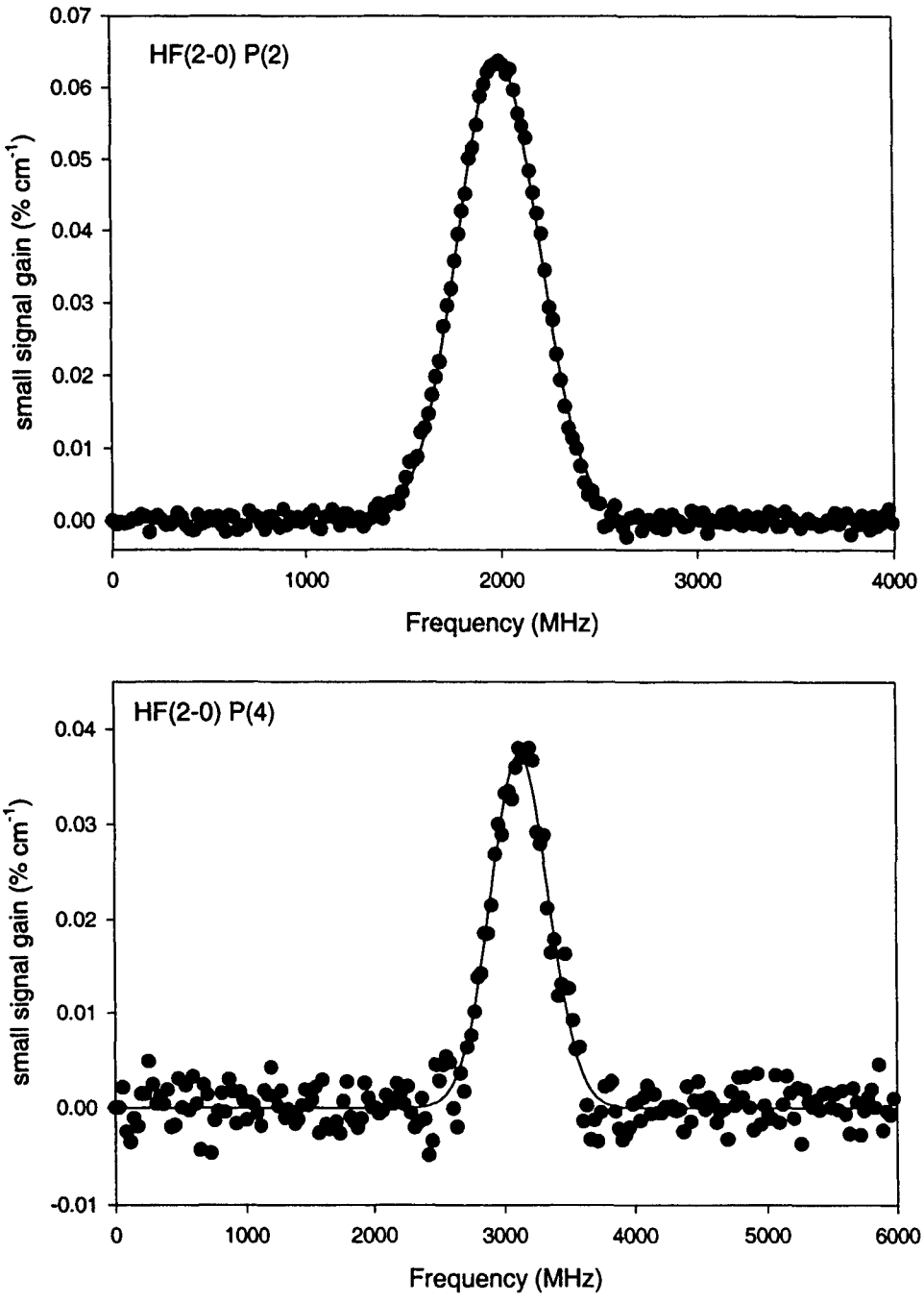

Figures 5 a - b. Small signal gain for HF(2-0) P(2) and P(4). In addition to measuring the small signal gain on HF(2-0) P(3), the diode laser can scan across several other overtone ro-vibrational lines. The HF(2-0) P(2) and P(4) lines are shown in the upper and lower panels, respectively. The experimental conditions for the upper panel are F_2 = 1 mmol sec^{-1}, H_2 = 27 mmols sec^{-1}, P ~ 2 Torr, x = 5 cm downstream of the NEP, and y = 0.25 cm above the centerline. The Gaussian function fit to P(2) spectrum corresponds to area = 33.4, linewidth(FWHM) = 490.3 MHz, and peak gain = 0.064 % cm^{-1}. The experimental conditions for the lower panel are F_2 = 1 mmol sec^{-1}, H_2 = 27 mmols sec^{-1}, P ~ 2 Torr, x = 1 cm downstream of the NEP, and y = 0.4 cm above the centerline. The Gaussian function fit to P(4) spectrum corresponds to area = 20.8, linewidth(FWHM) = 523.8 MHz, and peak gain = 0.037 % cm^{-1}

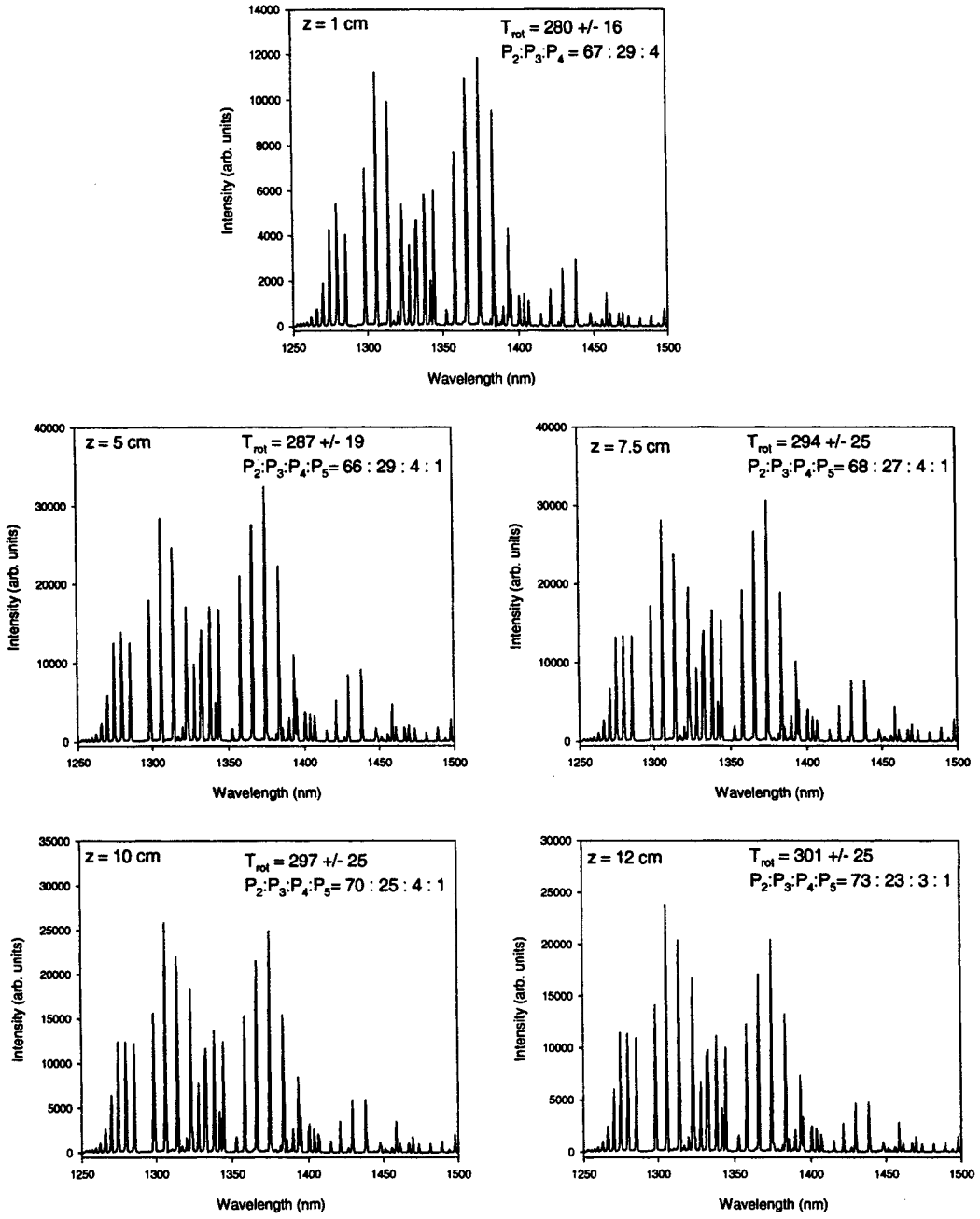

Figures 6a - e. HF overtone emission spectra. A Near Infrared Optical Multi-channel Analyzer (NIR OMA) was used to collect the HF overtone spectra shown above. Using fiber optic delivery to the monochromator, spatially resolved emission spectra can be generated. A Boltzmann analysis of the overtone spectra (see text) shows that rotational equilibrium has been achieved, that the rotational temperature increases slightly and the vibrational distribution relaxes as the flow progresses downstream. The experimental conditions for all panels are F_2 = 1 mmol sec^{-1}, H_2 = 27 mmols sec^{-1}, and P ~ 2 Torr. Although the fiber optic lens collects chemiluminescence from a small solid angle, it was positioned such that the entire vertical profile is observed simultaneously (y = centerline ± 0.5 cm).